ASSESSMENT OF STRUCTURAL EFFECT OF SELECTIVE STITCHING ON COMPOSITE SKIN-STIFFENER BONDING

Peter Linde*, Norbert Heltsch*, Lucie Chapelle, Jürgen Filsinger*****
***Airbus Operations GmbH, **INSA de Lyon, ***EADS IW**
peter.linde@airbus.com; norbert.heltsch@airbus.com; lucie.chapelle@insa-lyon.fr; juergen.filsinger@eads.net

Keywords: *composite, stitching, disbonding, analytical model, experimental tests*

Abstract

Potential increase in structural efficiency may be obtained by improving the out of plane behavior in composite lightweight design.

Various 3D reinforcement technologies such as through the thickness stitching through multiple laminates have been studied since over 30 years with varying results.

Focus has often been placed on aerial stitching, and although a certain improvement in 3D strength could be reached and damage tolerance could be improved, a loss in the in-plane properties was generally observed. This was often not insignificant, and is unfortunate, since it has a direct effect on the important tensile, compressive and flexural behavior.

Recent research has suggested that stitching in only selected areas may be sufficient in order to provide certain positive effects, whereas some of the main drawbacks may be reduced. In order to investigate this, some simple experimental testing and corresponding theoretical studies have been carried out.

The aim is to study the effect of a single reinforcement seam of stitches along the edge of a stiffener foot on the skin/stiffener bonding.

The foot of the stiffener is represented by a doubler, thus the web is being left out in this study. The study of flexural behavior perpendicular to the stiffener main direction is carried out by 3-point bending tests.

A simple analytical model is developed for prediction and for selecting the parameters of the tests. Due to complex behavior around the stitch yarn, simplified model assumptions had to be made.

Different parameters of the selective stitching such as skin thickness, stitching type and pitch are considered. Comparison between experimental and analytical estimations is performed. Finally conclusions and recommendations for future research are presented.

1 Introduction

Composite lightweight design currently has a high priority in aeronautical research.

Potential increase in structural efficiency may be obtained by improving the out-of-plane behavior. Technologies to reach this include 3D reinforcement within laminates, and various types of through the thickness pinning and stitching through multiple laminates.

In the latter case, focus has often been placed on aerial stitching, i.e. with stitch channels placed in a square pattern of a certain pitch. Usually it could be shown that a certain increase in 3D strength could be reached and that damage tolerance could be improved.

However, both characteristics could mainly be reached when the aerial pitch was below a particular value, i.e. the stitching was "dense" enough. The drawback has practically generally been a loss in the in-plane properties, as the "prize to pay" for the improvement in the out-of-plane direction. This was often not insignificant, and this is unfortunate, since it has a direct effect on tensile, compressive and flexural behavior [1]

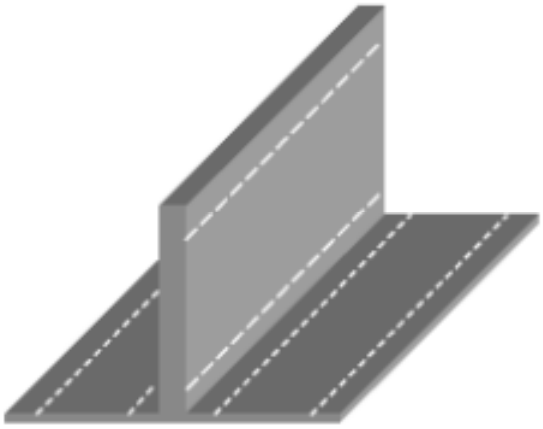

Fig. 1. Selective stitching of stiffener with single seams, from Baisch [2]

Recent research has suggested that stitching in only selected areas may still have limited but positive effects, potentially without displaying the severe in-plane adverse effects discussed above.

An early example of this approach is exemplified by Baisch [2], who in 2004 worked on stiffened panels with the stiffeners selectively stitched to the skin.

Fig. 2. Selective stitching of stringers on curved panel, from Baisch [2]

The work focused on stitching of single seams along the edges of stiffener feet, through both stiffener foot and skin, and another seam in the foot near the web, as well as two seems in the web, see figure 1. In [2] a variety of stitching types, such as tufting, single-sided stitching etc. were tested at the CTC (Composite Technology Center) in Stade.

The research also comprised extensive manufacturing related trials ranging from tools, studying tool stiffness to support the dry preform as well as permitting stitch needles to enter into the tool without damaging the needle, fixation of the component during stitching and the infusion process.

Figures 3 and 4 show the basic principle of tufting (using a straight needle) and single sided blind stitching (using a curved needle), as used in this study, both from the stitching head- and

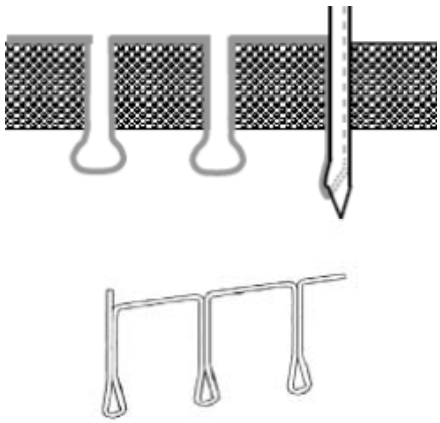

Fig. 3. Tufting, from Baisch [2]

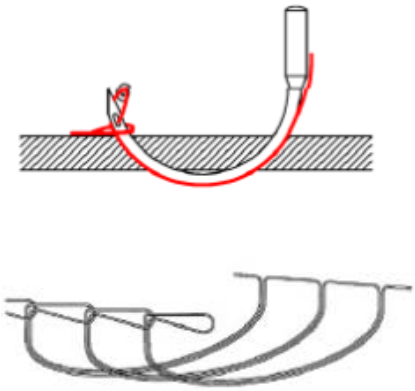

Fig. 4. Single sided blindstitch, from Baisch [2]

needle manufacturer KSL (Keilmann Sondermaschinenbau), located in Lorsch.

Further notable research within this general approach has been carried out by Velicki et al [3, 4] and Jegley [5], drawing upon extensive experience originating from the McDonnell Douglas Phantom Works. In this research interesting damage arresting capabilities such as crack turning effects as well as beneficial fatigue behavior have been studied. This work has been continued and expanded and is currently ongoing, recently represented in [6].

2 Coupon manufacturing

Amongst the several potential benefits that may be achieved by selective stitching, focus has been placed on the effect on the attachment between stiffener and skin in stiffened panels. If the bond between the foot of the stiffener and the skin can be improved this will be beneficial for the integrated structural behaviour of the stiffened panel not at least for buckling.

In order to study the effect on the stiffener foot bonding to the skin, the behaviour of an assembly across the length of the stiffener is considered. For experimental tests, a specimen consisting of a plate, representing the skin, bonded with a doubler strip, representing the foot of a stiffener, are considered. Thus the web of the stiffener is left out in these tests. Focus is placed on the effect on the bonding of single stitching seams, placed through skin and doubler, near each edge of the doubler.

In figure 5 a corresponding test specimen is shown, devised as a 3-point bending test. The length of the specimen is 200 mm, the width is 100 mm (up from standard 20 mm, in order to have 10 stitches across width, with pitch of 10 mm). The length of the doubler is 60 mm.

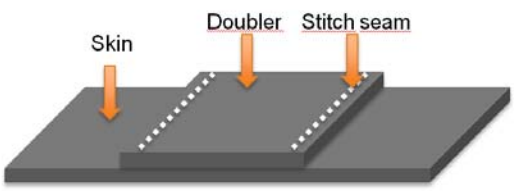

Fig. 5. Three point bending specimen

Fig. 6. Cut NCFs in waiting of layup

A series of specimens have been built and tested [7]. The parameters involved were the skin and the doubler thickness, the stitch seam type (tufting and singled sided blind stitch) as well as the stitch pitch, and the yarn thickness.

The skin and doubler were built of the identical material, consisting of noncrimp fabrics, of the type Saertex Quadrax 510 gsm, consisting of four plies together having a 0,5 mm thickness. Culimeta E-Glass yarn with specific weight of 34 and 68 tex, respectively, was employed.

Figure 6 shows non crimped fabrics cut to size awaiting layup in the process of the specimen building.

Figure 7 shows ongoing tufting of a specimen with the doubler face down. Correspondingly figure 8 shows blind stitching of a specimen. The curved needle should be noticed.

Fig. 7. Tufting of a specimen with doubler face down

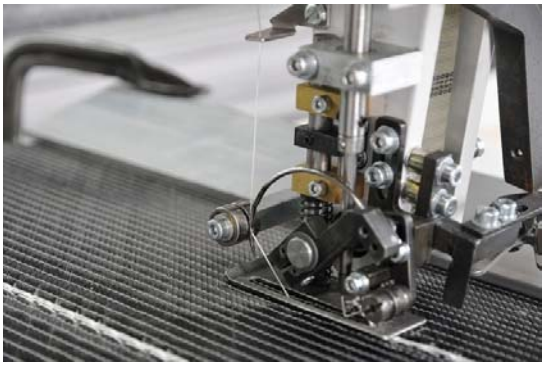

Fig. 8. Blind stitching of a specimen – notice curved needle

3 Experimental testing

The three point bending test is shown in Figure 9, including the test rig, and a mounted specimen. The test rig consists of a centrally acting hydraulic cylinder with load cell. The specimen is mounted, doubler facing down, resting on two semi circular supports of the same shape as the one in center with which the load is applied.

The load is placed along the centre of the doubler, representing a load from the web which is not present on these specimens, for simplicity, since focus in this study is placed on the effect of the seam at the edge of the doubler.

Tests were carried out with displacement controlled center load, with readings of load and measurement of the center displacement. Test results in the form of load displacement curves are displayed in the figures 10 through 17, which each have an unstitched specimen as base line. The distance between the supports measures 120 mm, and the remaining 30 mm to the end of the specimen was needed since the anticipated ductility of the stitched specimens being high, a risk of the specimen edge slipping over the support was considered.

It is noticed from figures 10 and 11 that the effect of the single stitching seams is relatively limited in terms of force and ductility. The steep fall in the curve for the unstitched specimens indicates laminate failure. The first steep fall in the curves for tufted/stitched specimens indicates yarn failure. For the heavier yarn grade 68 tex there is a limited but clear load increase of some 10 % and a ductility increase of some 20-25 %. For the lighter yarn there is hardly any force improvement; and this is in line with reports on experience with tufting on thin

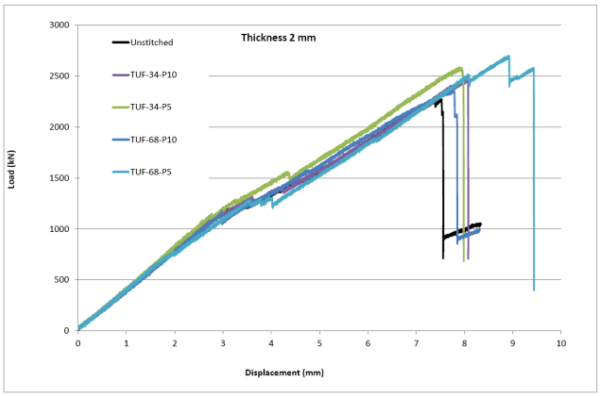

Fig. 10. Load – displacement curves for tufted specimens with 2 mm skin thickness

Fig. 9. Skin-doubler 3 point bending specimen in test rig [6]

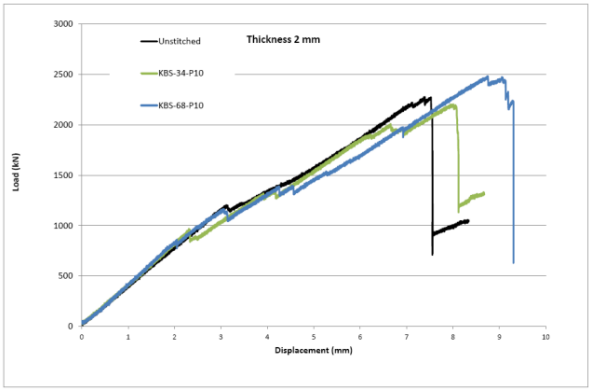

Fig. 11. Load-displacement curves for blind stitched specimens with 2 mm skin thickness

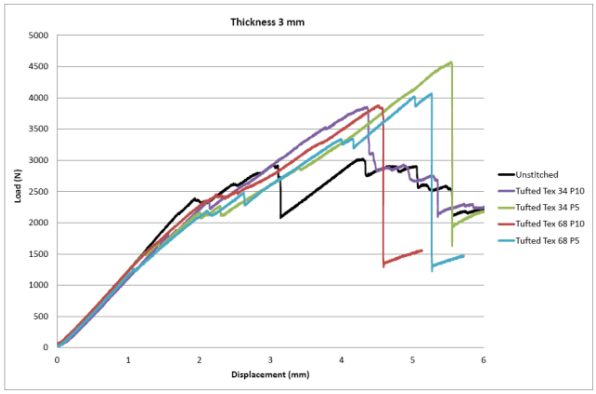

Fig. 12. Load displacement curves for tufted specimens with 3 mm skin thickness

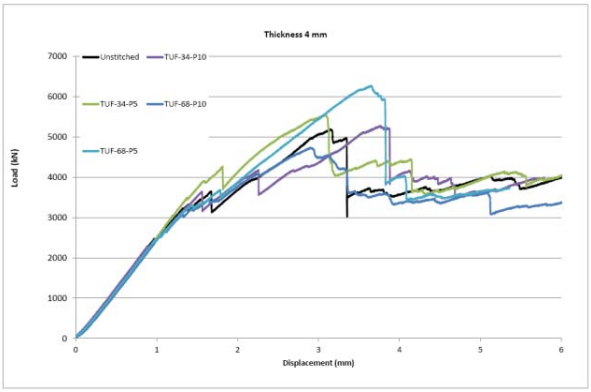

Fig. 14. Load-displacement curves for tufted specimens with 4 mm skin thickness

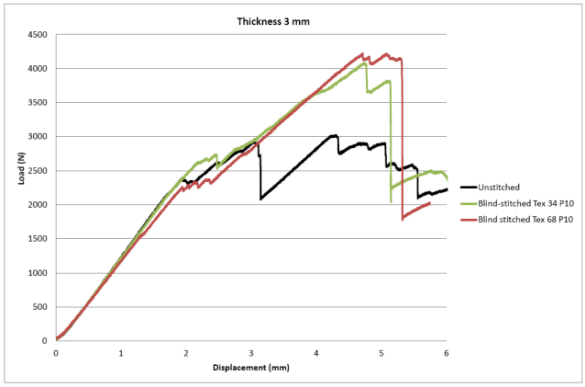

Fig. 13. Load-displacement curves for blind stitched specimens with 3 mm skin thickness

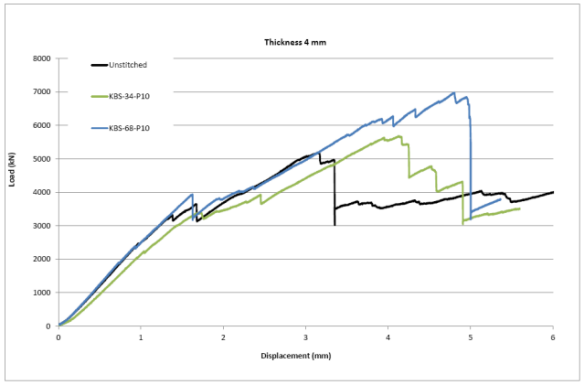

Fig. 15. Load-displacement curves for blind stitched specimens with 4 mm thickness

laminates; the bonding area of the tufts is limited, and the friction may be limited. No major difference could be observed in effect between tufting and stitching.

The effects for the specimens with 3 mm skin thickness are already considerably better, as seen in figures 12 and 13. Tufting results in an average appr. 25 to 30% load increase and 50 to 70 % ductility increase. The effects for blind stitching are even somewhat larger; with appr. 40 % load increase and up to 80 % ductility increase.

The effects in the 4 mm thick specimens, of figures 14 and 15 are good with the exception of some of the tufted specimens. Cross sectional examination revealed incorrect internal laminate geometry right at the stitch channels and incorrect stitch channel geometry, which shows that utmost care needs to be taken. These specimens will be rebuilt and retested.

Figures 16 and 17 finally reveal in general good effects for the 5 mm thick specimens, although a decreasing trend may be observed at these high laminate thicknesses.

In summary; for the thinnest laminates only 68 tex yarn provides some improvement, from 3 mm thickness and up already 34 tex provides clear load increase and excellent ductility improvement.

This holds in general for thicker laminates with a certain decreasing trend. The method appears sensible to irregularities in laminate and stitch tolerances, which needs to be further confirmed. Further studies should be carried out, such as separate Mode I and II tests as well as study of effects along length of stiffener acc. to [8].

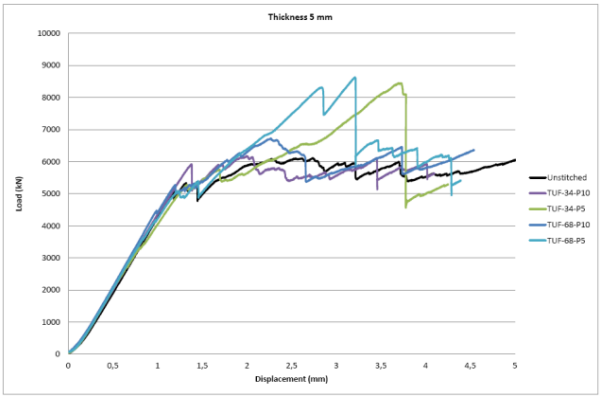

Fig. 16. Load-displacement curves for tufted specimens with 5 mm skin thickness

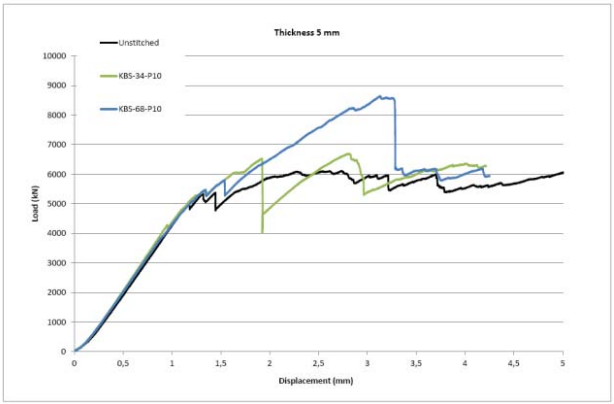

Fig. 17. Load-displacement curves for blind stitched specimens with 5 mm skin thickness

4 Analytical Model for Tufting

In order to estimate the order of magnitude of forces, deformations etc. to expect during the tests and not at least to enable an estimation of the parameters in the test matrix, it was considered to set up a theoretical calculation.

Assessing the stitch geometry of tufting and blind stitch, see figures 3 and 4, it was decided to first focus on tufting, due to its straight geometry. Due to the known complex physical mechanisms involving the functioning of a stitch yarn, undergoing different phases of damage, such as undamaged bond around the yarn, partial disbonding of the , subsequent stretching of the yarn, potential mixed mode mechanisms involving normal and shear mode, friction, and finally; fracture of yarn, it was decided to stay with an approximate analytical model on the “macro level” mainly focusing on the most important behavior in transferring of forces, for the simplest of the stitch types; the tufting, [9].

The basics of the model are shown in figure 18. On top is shown a front view of the three point bending assembly, with the load introduction from below on center, and the support rolls at the sides. The tufting yarns are displayed at the edges of the doubler as dotted lines.

The mid figure shows the right half of the assembly, under the simplified assumption of symmetry in the assembly middle (at load introduction). The bottom figure introduces the assumption of a disbonding crack between the doubler and the skin which is starting from the doubler edge and at some point passing through the tufting seam and that propagates inward towards the center. Thus this is a simplified “ultimate” state in which the yarn carries the full force transfer.

Figure 19 depicts how the bottom assembly of figure 18 looks like in terms of deformed

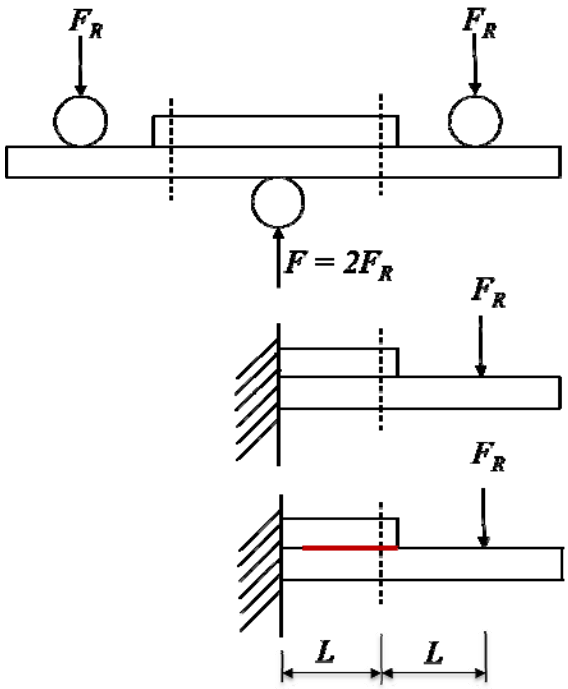

Fig. 18. Analytical model for 3-points bending test specimen with assumption of full disbonding between skin and doubler

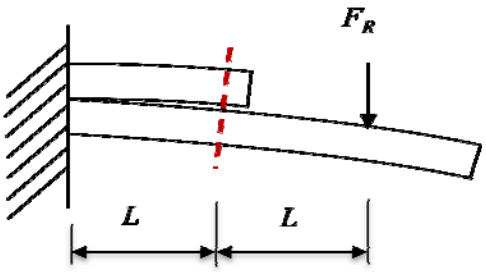

Fig. 19. Deformed shape, showing disbonding opening, held back by yarn only

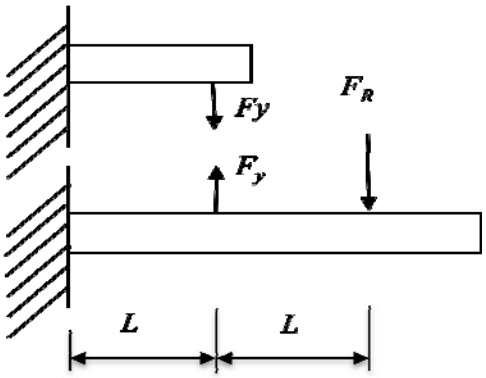

Fig. 20. Force acting on parts of de-bonded skin-doubler

shape. Hereby it is seen that the yarn takes the whole force transfer between skin and doubler. Figure 20 displays the forces, including the yarn forces, acting. Regarding the doubler only, it acts essentially as a cantilever beam.

For a given specimen geometry, i.e. given L, and given yarn properties, and given stitch/tufting pitches (5 mm and 10 mm) the first task was to seek reasonable laminate thicknesses for the tests.

This can be done by assuming ultimate flexural strain at the left end of the doubler, i.e. the laminate would break at this state. At the same time the yarn's full strength is assumed, here at first in a mode I, i.e. tension only, at the location of force *Fy*. This is a configuration which would give simultaneous laminate failure and yarn failure. Thus, all smaller thicknesses should result in laminate failure, and all larger thicknesses should result in yarn failure.

With the following simplifying assumptions made:

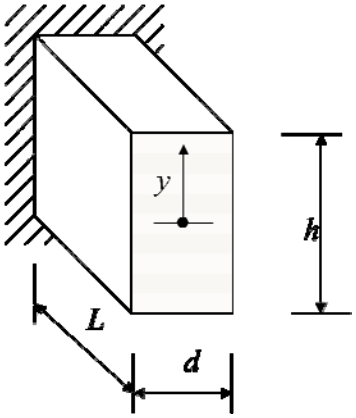

Fig. 21. Laminate cross section with unit width

- No premature local skin buckling
- Quasi isotropic fabrics
- Practically a full breakage of the resin between doubler and skin
- Symmetry permitted
- No shear displacement between skin and doubler considered

the first use of the analytical model; the sequence for finding the range of the laminate thicknesses for the tests, is summarized here as follows

$$M = F_y L \qquad (1)$$

In which M is the bending moment at the base of the doubler cantilever, see figure 20, F_y is the force in the stitching yarn, and L is the length of the cantilever to the yarn.

$$\sigma = \frac{My}{I} \qquad (2)$$

in which σ is the stress at the outermost fiber, on the distance y from the centroid, and I is the moment of inertia for the laminate cross section, see figure 21.

$$I = \frac{dh^3}{12} \qquad (3)$$

in which d is the width of the cross section regarded (here a "unity" width is assumed), and h is the laminate height (thickness).

$$\sigma = E\varepsilon \qquad (4)$$

in which E is laminate Young's modulus, and ε is the strain. Equating expressions (1), (2) and (3) results in:

$$\frac{12F_y Ly}{dh^3} = E\varepsilon \qquad (5a)$$

and resolving for F_y:

$$F_y = \frac{E\varepsilon dh^3}{12Ly} \qquad (5b)$$

This expression thus relates the yarn force to the laminate Young's modulus, flexural strain, to the laminate thickness, and cantilever length. For this equation (5b) may be rewritten as:

$$F_y = \frac{E\varepsilon dh^3}{12L_1\frac{h}{2}} = \frac{E\varepsilon dh^2}{6L_1} \quad (6)$$

and solving for h^2 yields:

$$h^2 = \frac{6F_y L_1}{E\varepsilon d} \qquad (7)$$

Thus, inserting in eq. (7) known constants and for F_y stitch yarn properties and stitch pitch, divided over the used unit width here, the field of laminate thicknesses could be determined. It resulted in a series of thicknesses starting at 2 mm in steps of 1 mm up to 5 mm.

With the above, the max yarn forces are estimated in a pure mode I i.e. only normal yarn action. This provides an overestimate of the yarn forces, since the test also inflicts shear action at the doubler edge, and in order to obtain a more realistic level of prediction it is necessary to assess simple mixed mode behaviour, extending the model above, summarized in the following.

The kinematics of the modes I (normal) and II (shear) are introduced. Starting with pure model I and regarding the behaviour in the laminate, we see in figure 22 that after the interlaminar disbonding crack, between skin and doubler, has passed, starting that edge, propagating across the yarn, some disbonding damage starts around the yarn from the interlaminar disbonding crack and propagates into the depth of the laminate, thus leaving a damaged zone around the center.

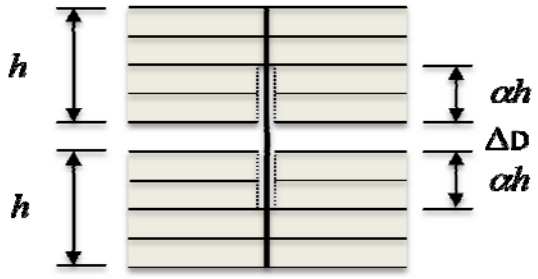

Fig. 22. Laminate in pure mode I with damaged bonding of yarn

Assuming disbonding of yarn occurs over a fraction α of the laminate thickness h, see figure 21, the total de-bonded yarn length is

$$L_y^{db} = \alpha h + \Delta D + \alpha h \qquad (8)$$

and with the failure strain of the yarn ε_b, we obtain

$$\Delta D = L_y^{db} \cdot \varepsilon_b \qquad (9)$$

as an estimate of max normal displacement between the laminates.

In a mixed mode case like here this will not be reached since the shear displacement contributes significantly and thus the mode II mechanism must be regarded as well.

Figure 23 shows a schematic view of the mixed mode behaviour in an ultimate state, the yarn seen in detail in figure 23.

Estimation of the shear displacement ΔS can be made by integrating the strain of the top fibre of the laminate over the length of the symmetric doubler, assuming laminate failure strain on the left end and zero strain on the right end.

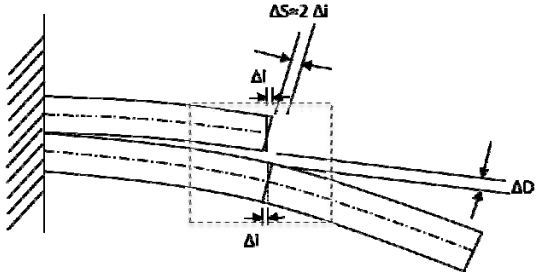

Fig. 23. Combined mode I and mode II kinematics at ultimate state

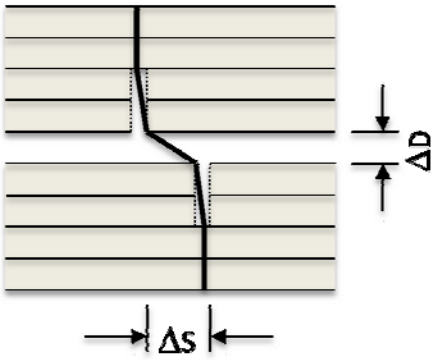

Fig. 24. Yarn mechanism at combined load

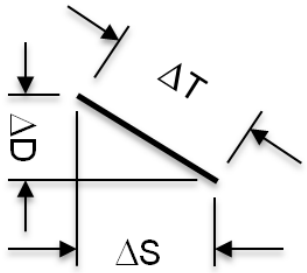

Fig. 25. Kinematic contributions for yarn criterion

An enlargement of the area inside the dotted box is shown in figure 24, with a simplified kinematic view of the yarn.

It is seen here that the yarn is bonded in undamaged levels of the laminate, and towards the interface between the laminates, disbonding of the yarn has taken place. In between the laminates the oblique combined mode I and mode II behaviour is shown. Over the de-bonded length, the yarn may develop its full strain, until its failure strength is reached.

Assuming the main displacement along the length between the laminates it is possible to regard the contributions from mode I and mode II and construct a simple mixed mode yarn failure criterion, here based on displacement, under the assumption that the yarn behaves elastically until rupture, see figure 25:

$$\Delta T = \sqrt{(\Delta D)^2 + (\Delta S)^2} \qquad (10)$$

in which ΔT is the total yarn extension. For each skin thickness a relation of ΔS to ΔD can be found, and the force (yarn force F_y, corresponding in magnitude to support force F_r in figure 20), from eq. (6) for mode I only, i.e. corresponding to ΔD only, can be reduced by a reduction factor, taking both mode I and mode II into account, by letting ΔT reach the failure strain in eq. (10), occurring at a value for ΔD smaller than its separate failure level.

Thus, force are estimated analytically for tufting, by doubling the value from eq. (6) and taking the mixed mode into account by using eq. (10) setting ΔT to failure level, having assumed α to 0,5 (for all skin thicknesses, and solving for ΔD knowing ΔS/ΔD. The results for 3 mm skin thickness and tufting are seen in figure 26, where the analytical estimates are plotted with the test results. The result is slightly conservative for yarn grade 68 tex with the force level predicted to appr. 90 % of test. For yarn grade 34 tex it is more conservative with a prediction of appr. 65 % of test. Factors to in-

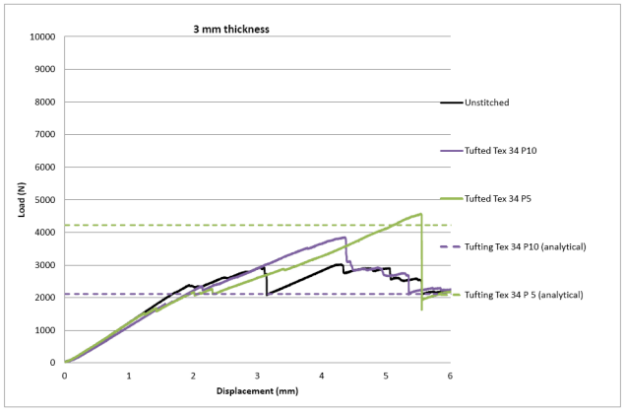

Fig. 26. Analytical predictions by model for tufting with tufting results

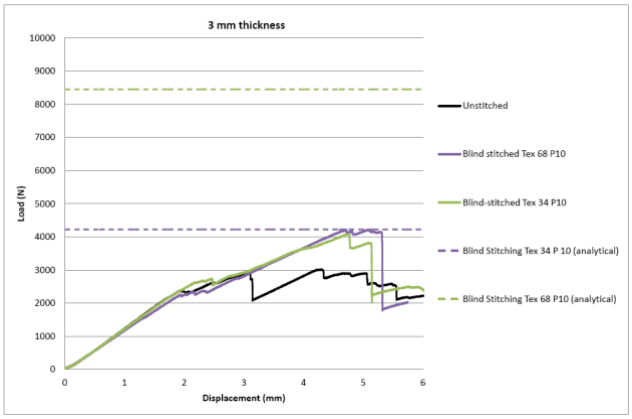

Fig. 27. Analytical predictions by model for tufting with blind stitch results

vestigate here range from: ratio α and its potential dependence of yarn grade, friction at the "corners" seen in figure 23 may play a role, and a more refined criterion than in eq. (10) may be possible to construct already by more precisely taking the yarn geometries in figure 23 into account.

Inadequacy to use the models derived for tufting on blind stitched specimens is seen in figure 27 in which over prediction occurs for 68 tex, although for 34 tex the force practically matches the test. The geometry of blind stitch, seen in figure 4, suggests that a more adequate model may have to be developed for that stitch pattern.

5 Conclusions and recommendations

The experimental tests in this study were limited, and only comprised 3-point bending tests. They are considered realistic though. Their mixed mode mechanism, is however not easy to model and simulate realistically and efficiently.

The following conclusions can be drawn based on the tests:

- In general a very clear beneficial effect could be observed in terms of structural behaviour on the selectively stitched specimens compared to the unstitched; in particular:
- Ductility increased significantly in most specimens, with increases of up to 50 % to at the most 80 % improvement vs. unstitched. This ductility increase may be interesting for buckling behaviour
- For the thinnest skin thickness tested here, 2 mm, the effects were clearly reduced compared to the higher thicknesses, likely due to limited bonding area between yarn and resin
- For the largest skin thickness tested here, 5 mm, the effects were somewhat reduced compared with e.g. 3 mm, likely due to the increasing relative importance of the unstitched structure's own mechanism

The following recommendations are made:

- Further studies should be made involving pure mode I and mode II tests
- Effects along stiffener length should be studied by larger test articles
- Effect of selective stitching on in-plane behaviour should be studied
- The analytical model shown here should be improved, and influence of factors such as mentioned in Ch. 4 should be studied
- A similarly simple model should be considered for blind stitch
- FE models, potentially based on the concept shown here, started in [10], should be further considered.

References

[1] Dell'Anno, G., *Effect of tufting on the mechanical behaviour of carbon fabric/epoxy composites*, Ph.D. thesis, Cranfield University, 2007

[2] Baisch, P. *Nähtechnische Montage und Modifizierung eines faserverbundverstärkten Rumpf-schalen-Segments im Kontext einer hoch automatisierten Prozesskette*. M.Sc. thesis. CTC, Stade, July, 2004

[3] Velicki, A. Blended Wing Body Structural Development, *Proc. Royal Aero-nautical Society First Structural Design Conf.*, London, 2008

[4] Velicki, A. Damage Arrest Design Approach using Stitched Composites, *Proc. Royal Aeronautical Society 2nd Structural Design Conf.*, London, 2010

[5] Jegley, D. Experimental Behavior of Fatigued Single Stiffener PRSEUS Specimens, NASA/TM-2009-215955, 2011

[6] Bergan, A., J. G. Bakuckas, Jr., A. Lovejoy, D. Jegley, K. Linton. Full-Scale Test and Analysis of a PRSEUS Fuselage Panel to Assess Damage-Containment Features, FAA techn paper, 2011

[7] Heltsch, N. *New structural shell concept of improved damage tolerant design contributing to robustness, post-buckling and large damage capabilities for a 2nd generation CFRP fuselage*, Internal Memo, Airbus, 2011

[8] Petiot, C. ALCAS-2.3.3 *Curved panels, post buckling capabilities, Bonding joints, disbonding criteria*, Technical report, 2010-42004-1-IW-SP, EADS-IW-F, 2010

[9] Linde, P. Preliminary Analytical Assessment of Effect of Selective Stitching on Stringer Foot Disbonding, Technical report, RP1123638, Airbus, 2011

[10] Boucher, C. Numerical prediction of the structural behaviour of selectively stitched composite coupon specimens, Technical Report, RP1128707, Airbus, 2011

Copyright Statement